Cell, Vol. 119, 33–45, October 1, 2004, Copyright ©2004 by Cell Press

# Architecture of the Hin Synaptic Complex during Recombination: The Recombinase Subunits Translocate with the DNA Strands

**Gautam Dhar,[1] Erin R. Sanders,[1] and Reid C. Johnson[1,2,*]**

[1]Department of Biological Chemistry
David Geffen School of Medicine
[2]Molecular Biology Institute
University of California, Los Angeles
Los Angeles, California 90095

## Summary

**Most site-specific recombinases can be grouped into two mechanistically distinct families. Whereas tyrosine recombinases exchange DNA strands through a Holliday intermediate, serine recombinases such as Hin generate double-strand breaks in each recombining partner. Here, site-directed protein crosslinking is used to elucidate the configuration of protein subunits and DNA within the Hin synaptic complex and to follow the movement of protein subunits during DNA strand exchange. Our results show that the protein interface mediating synapsis is localized to a region within the catalytic domains, thereby positioning the DNA strands on the outside of the Hin tetrameric complex. Unexpected crosslinks between residues within the dimerization helices provide evidence for a conformational change that accompanies DNA cleavage. We demonstrate that the Hin subunits, which are linked to the cleaved DNA ends by serine-phosphodiester bonds, translocate between synapsed dimers to exchange the DNA strands.**

## Introduction

Site-specific DNA recombination reactions control a diverse array of biological reactions including gene transcription, integration and excision of viral DNA from host chromosomes, assembly of genes from disparate gene fragments, resolution of chromosome or plasmid dimers, control of plasmid copy number, and transposition of DNA (Craig et al., 2002). Most site-specific recombination systems can be classified into two mechanistically and structurally distinct classes: serine and tyrosine recombinases. Recent atomic structures, combined with years of biochemical dissection, demonstrate that the tyrosine recombinases catalyze recombination by two sequential single-strand cleavage-ligation steps involving tyrosine-DNA phosphodiester linkages and the formation of a Holliday structure DNA intermediate (Jayaram et al., 2002; Rice, 2002; Van Duyne, 2002). In contrast, serine recombinases generate double-strand DNA breaks resulting from a near-concerted attack by a pair of serine hydroxyls on the recombinase dimer, and DNA exchange can proceed in an iterative manner whereby multiple exchanges of both strands occur within a single synaptic complex (Grindley, 2002; Johnson, 2002). Moreover, an X-ray structure of a serine recombinase dimer bound to DNA (Yang and Steitz, 1995) bears no resemblance to the structure of tyrosine recombinases.

Hin is a member of the DNA invertase subclass of serine recombinases (Johnson, 2002). Hin controls flagellin gene expression in *Salmonella enterica* by catalyzing inversion of a 1 kb regulatory segment of the chromosome (Silverman et al., 1981; Zieg et al., 1977). The native Hin-catalyzed inversion reaction requires the presence of the Fis regulatory protein that controls the activity of Hin when bound to a remote recombinational enhancer DNA segment (Johnson et al., 1986; Johnson and Simon, 1985). Recombination occurs in the context of an invertasome complex containing the two *hix* recombination sites bound by Hin dimers and the enhancer bound by two Fis dimers on a supercoiled DNA molecule (Figure 1A) (Heichman and Johnson, 1990; Johnson et al., 1987). These regulatory complexities ensure that only intramolecular inversions of DNA between *hix* sites are catalyzed.

A gain-of-function mutant of Hin that contains a histidine to tyrosine substitution at residue 107 can promote intermolecular recombination in the absence of the enhancer, Fis, HU, or DNA supercoiling (Sanders and Johnson, 2004). Under metal-free reaction conditions, Hin-H107Y forms stable synaptic complexes assembled from four protomers of Hin and two *hix* DNA fragments, with each Hin subunit covalently linked to the 5′ end of the cleaved *hix* site through a serine-phosphodiester bond (Figure 1B). The DNA strands within these intermediates can be ligated into either the recombinant or parental configurations upon addition of $Mg^{2+}$. The Hin-H107Y hyperactive mutant therefore provides a means to explore the structure of the catalytic core and the mechanics of DNA exchange in a simplified reaction.

The structure of Hin bound to the 26 bp *hix* site has been modeled based on crystal structures of the γδ resolvase catalytic and Hin DNA binding domains (Figure 1C) (Chiu et al., 2002; Haykinson et al., 1996; Johnson, 2002; Rice and Steitz, 1994b; Yang and Steitz, 1995). The Hin and γδ resolvase catalytic domains share 40% identical/63% similar residues, and protein folding programs indicate a good correspondence between the modeled Hin and resolvase X-ray structures, except for residues 27–36, where some ambiguity exists. The model is considered to be a catalytically-inactive apo-structure, since the active site serine 10 residues are not sufficiently close to the DNA to attack the phosphodiester backbone, and the C-terminal ends of the coiled-coil dimerization helices (E helices) block the approach of the serines toward the DNA. Thus, a change in the recombinase structure is likely to be a prerequisite for DNA cleavage (see Yang and Steitz [1995]). The region of Hin that mediates synapsis, the nature of the conformational changes that lead to coordinated cleavage of the four DNA strands (Merickel et al., 1998), and the mechanism by which the DNA strands are exchanged after cleavage are all poorly understood.

To address these issues, we have positioned cysteines within or near regions that potentially may form

*Correspondence: rcjohnson@mednet.ucla.edu

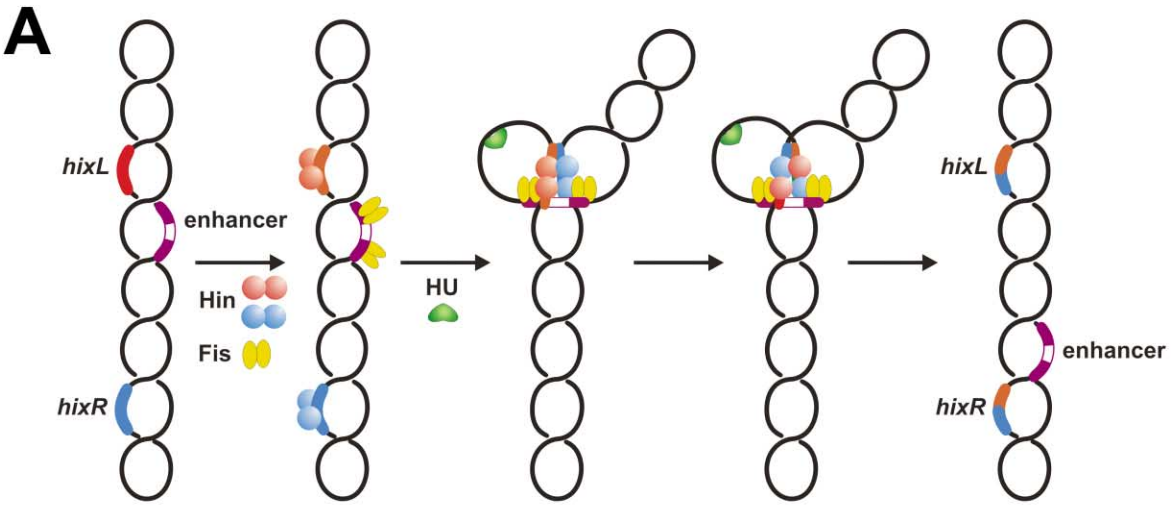
A
hixL
enhancer
Hin
Fis
hixR
HU
hixL
enhancer
hixR

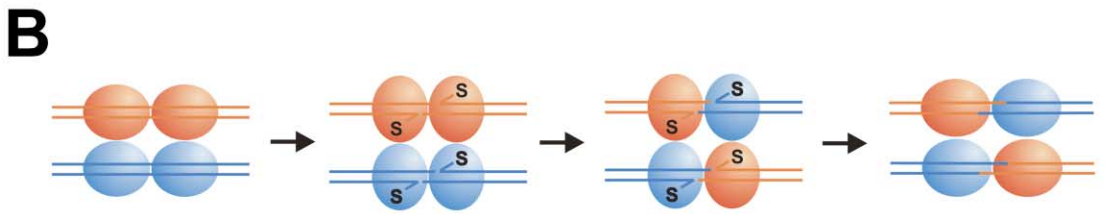
B
S

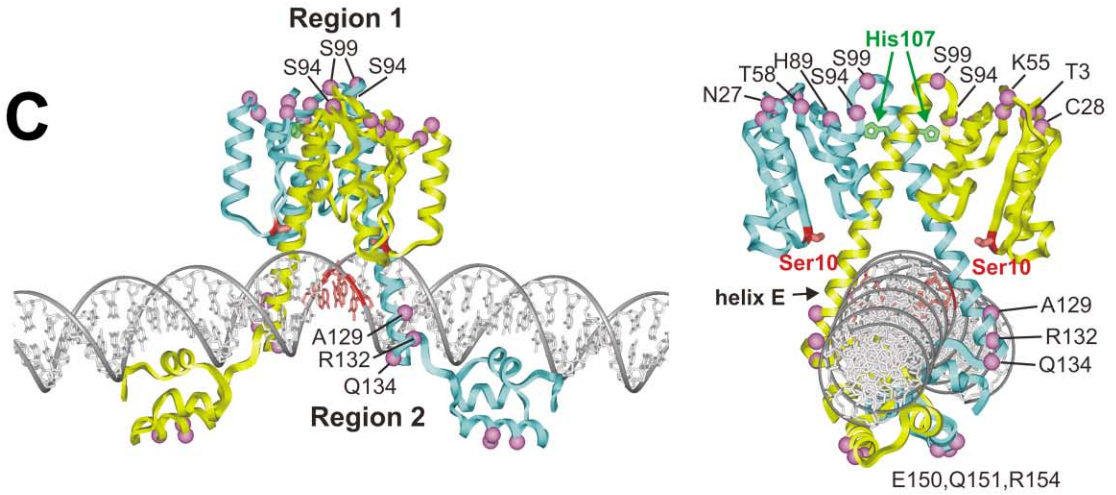
C
Region 1
S99
S94
S94
A129
R132
Q134
Region 2
His107
H89
S99
S99
T58
S94
S94
K55
T3
N27
C28
Ser10
Ser10
helix E
A129
R132
Q134
E150,Q151,R154

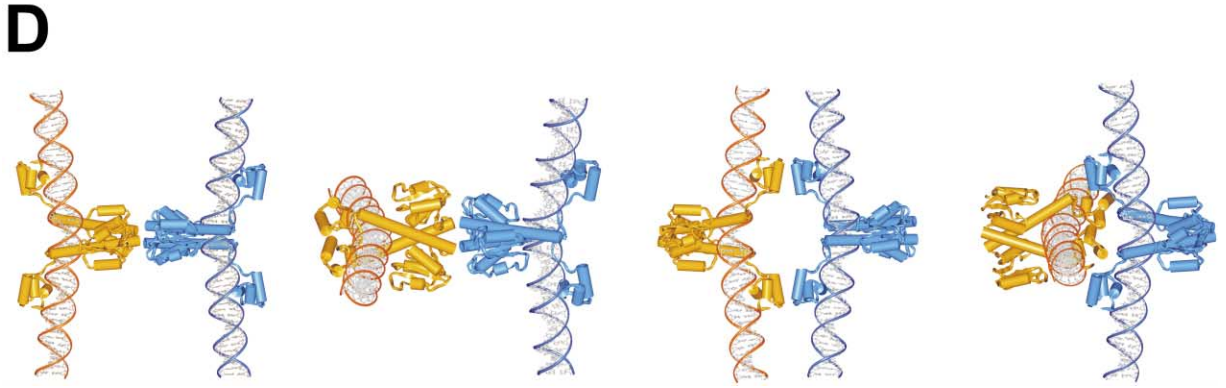
D

interfaces during the reaction. Chemical crosslinking using sulfhydryl-reactive reagents has enabled us to determine the location of the synaptic interface and model the configuration of protein subunits and DNA segments in the synaptic complex. Kinetic analyses of crosslinked products provide experimental support at the protein level for the recombination reaction involving exchange of Hin subunits together with the DNA strands.

## Results

### Crosslinking Strategy to Probe Protein Interfaces in the Synaptic Complex

Whereas a number of configurations for a tetrameric Hin synaptic complex are possible, two general classes of models, which are schematically represented in Figure 1D, appear the most structurally plausible. In one class, the DNA duplexes are located on the "outside" of the Hin synaptic tetramer in orientations ranging from parallel to perpendicular. Synaptic contacts between Hin dimers would be localized to the top region of the Hin catalytic domains, as oriented in Figure 1C, with the specific interacting surfaces reflecting the relative alignments of the catalytic domains. In the other class of models, the DNA duplexes are located on the "inside" of the Hin tetramer. In these arrangements, synaptic interactions stabilizing the tetramer would be mediated by residues within the DNA binding domains or at the base of the E helices. To distinguish between these configurations, predicted surface-exposed residues within potential interfaces were substituted with cysteines (Figure 1C), which could serve as unique sites for sulfhydryl-specific chemical crosslinking. Each of the cysteine-substituted Hin-H107Y mutants retained recombination activity and was able to form cleaved synaptic complexes with duplex oligonucleotide substrates.

Cleaved synaptic complexes assembled from 3′ $^{32}$P-labeled *hixL* oligonucleotides and cysteine-substituted Hin-H107Y mutants were separated from unreacted Hin and DNA in native polyacrylamide gels containing 10% glycerol (Figure 2A). Gel slices containing synaptic complexes were incubated with either diamide or DTNB to promote direct disulfide linkages, or *bis*-maleimide crosslinkers, which form covalent bridges between cysteines with linker lengths ranging from 8 to 18 Å ("in-gel" crosslinking). Alternatively, the reactions were crosslinked in solution prior to purification of synaptic complexes by gel electrophoresis ("in-solution" crosslinking). Hin-DNA complexes obtained from both methods were eluted from the gel and subjected to SDS-PAGE to separate the radiolabeled Hin-DNA conjugates. By gel purifying synaptic complexes and following the Hin that is linked covalently to the radiolabeled DNA, we are assured that any crosslinked Hin products reflect those assembled in a cleaved synaptic complex.

### Two Regions of Hin Support Efficient Crosslinking

Figure 2B shows representative results of in-gel crosslinking experiments with different cysteine-substituted Hin-H107Y mutants. In the absence of crosslinking, monomeric Hin protein is linked to the radiolabeled 17 nt DNA fragment comprising the 3′ segment of each strand of the 36 bp substrate after cleavage (lane 1 of each panel). Cysteine substitutions within two different regions of Hin generated crosslinked products. Region 1 is centrally located within the top surface of the catalytic domain. Within this region, Cys94 formed crosslinks with each of the crosslinkers used, including those generating direct disulfide bonds. Cys99 did not form disulfide bonds, but crosslinked Hin products were efficiently obtained using bridging crosslinkers. Region 2 is defined by Cys129, Cys132, and Cys134, which readily formed crosslinked products with the *bis*-maleimide crosslinkers (Figure 2B and data not shown). These residues are located at the C-terminal end of the E helices and, in the model of the Hin apostructure, are predicted to be on the opposite sides of the *hix* DNA prior to cleavage (Figure 1C). Crosslinked products were not observed with Hin-H107Y, which contains an endogenous cysteine at residue 28, or cysteines introduced at positions 3, 27, 55, 58, 89, 150, 151, and 154 (data not shown).

In-solution crosslinking experiments were performed to evaluate the rate of product formation. Cleaved syn-

Figure 1. Hin-Catalyzed Site-Specific DNA Recombination

(A) Pathway for site-specific DNA inversion on a supercoiled plasmid substrate by the Fis-dependent wild-type enzyme (Johnson, 2002). Hin dimers bind to the two recombination sites *hixL* and *hixR*, and Fis dimers bind to two sites on the 65 bp recombinational enhancer segment (magenta). The *hix* and enhancer DNA sites assemble into an invertasome complex at the base of a supercoiled branch with the help of the DNA bending protein HU. Hin becomes activated to cleave and exchange DNA strands within the invertasome complex. Consistent with data in this paper, Hin subunit exchange accompanies DNA exchange. The invertasome dissociates, resulting in an inversion of the intervening DNA between the *hix* sites.

(B) Pathway of recombination promoted by the Fis-independent mutant Hin-H107Y (Sanders and Johnson, 2004). Hin-H107Y binds to *hix*-containing oligonucleotides and assembles cleaved synaptic complexes in $Mg^{2+}$-free buffer containing ethylene glycol. Each of the four Hin subunits become bound covalently to the 5′ end of the cleaved DNA by a serine-phosphodiester linkage, and these complexes are competent for DNA exchange. The DNA ends ligate by reversal of the serine-phosphodiester linkage in the presence of $Mg^{2+}$ and dilution of the ethylene glycol, and the complexes dissociate into Hin bound DNA segments.

(C) Two views of the Hin dimer apostructure model bound to *hixL*. The Hin subunits are colored yellow and blue, with the side chains of the active site serine 10 shown in red and the gain-of-function mutation H107Y shown in green. Residues that were substituted with cysteine are depicted with magenta-colored spheres at their C$\alpha$ positions. Residues in regions 1 and 2 that support crosslinking are specifically labeled in the left panel. The core nucleotides at the center of the *hix* site, where Hin generates staggered cleavages with two base-protruding 3′ ends, are highlighted in red.

(D) Four possible configurations for the structure of Hin synaptic complex. In the left two models, synapsis is mediated by the catalytic domain, and the DNA strands are on the outside in a parallel or antiparallel orientation ranging up to perpendicular orientation. In the right two models, the DNA segments are in the inside of the complex in either parallel/antiparallel or perpendicular orientations. Different protein interfaces would be expected to stabilize the respective configurations.

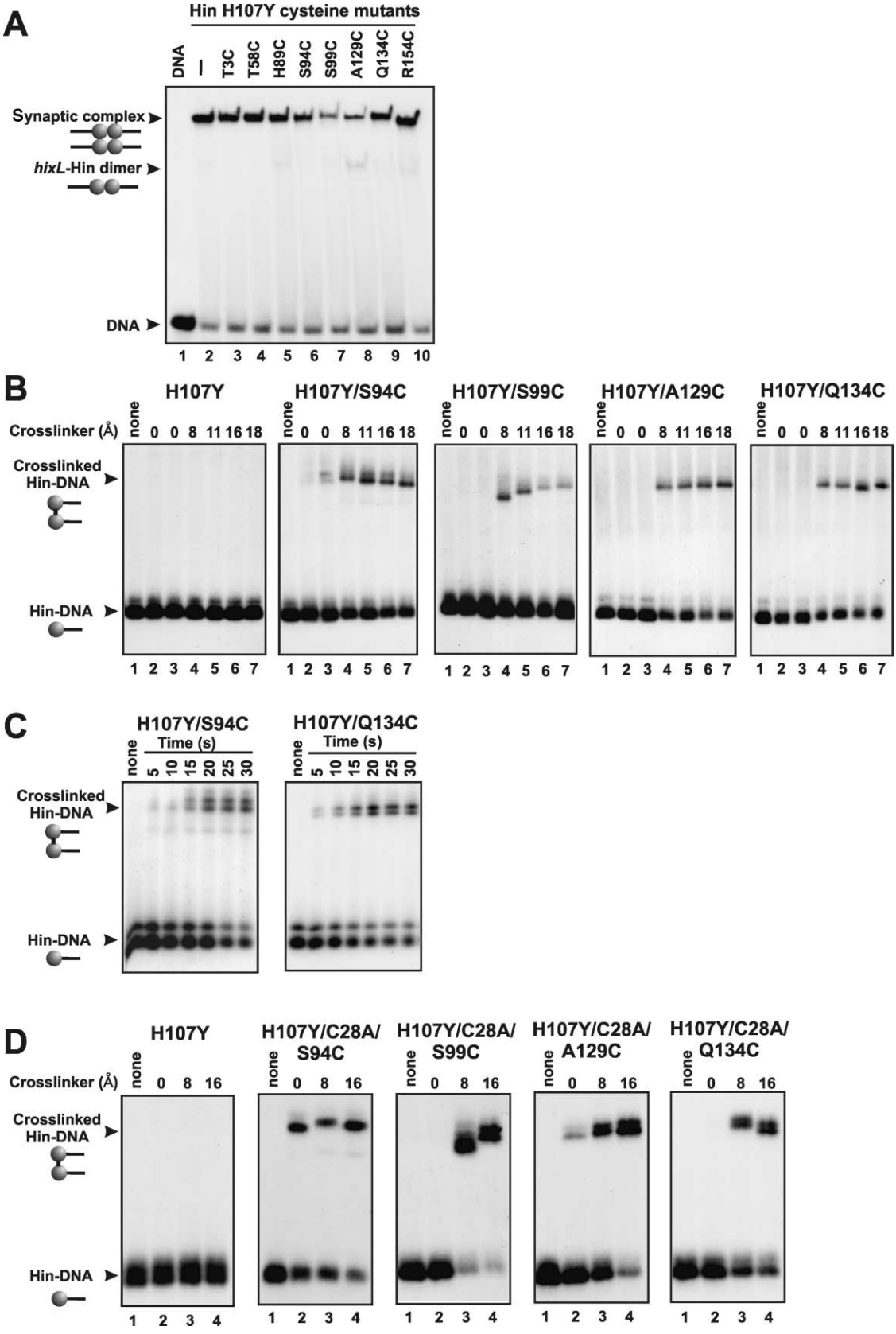


Figure 2. Crosslinking of Hin-H107Y Mutants Containing Cysteine Substitutions at Different Locations

(A) Isolation of Hin mutant synaptic complexes. Cleaved synaptic complexes were assembled using cysteine-substituted Hin-H107Y mutants and 3′ $^{32}$P-labeled 36 bp *hix* substrates and electrophoresed in a native polyacrylamide gel containing 10% glycerol. Under these conditions,

aptic complexes were assembled with Hin-H107Y/S94C or Q134C and subjected to crosslinking by BMOE (8 Å spacer) for time periods ranging from 5 to 30 s. As shown in Figure 2C, formation of crosslinked products is rapid, with substantial amounts of products generated after only a 15–20 s incubation with the crosslinker. In Figure 2D, cysteine-substituted Hin-H107Y mutants were exposed to different crosslinkers for 20 s. Each of these mutants lacked the endogenous Cys28. Hin mutants containing unique cysteines at positions 94, 99, 129, and 134 were efficiently crosslinked, whereas no crosslinked products were obtained with Hin-H107Y. Disulfide bonds formed readily between cysteines at position 94, and, unlike the in-gel crosslinking experiments, direct crosslinks between cysteines at position 129 were also obtained. Crosslinking with *bis*-maleimide reagents containing spacers of 8 or 16 Å was very efficient for each of the mutants containing cysteines in regions 1 and 2. The rapid kinetics and efficiency of crosslinking implies that these regions are in close proximity between subunits in the cleaved synaptic complex.

### Crosslinking Is Dependent upon Synaptic Complex Assembly

To confirm that the crosslinking only occurs in the context of the synaptic complex, Hin-H107Y proteins containing cysteines at positions 94 (region 1) and 134 (region 2) were $^{32}$P-labeled by means of a kinase tag introduced at their C termini. Hin-DNA complexes were assembled with unlabeled DNA substrates and separated in a native polyacrylamide gel (Figure 3A, lane 3). Bands corresponding to Hin dimers bound to single *hix* sites and tetrameric Hin synaptic complexes were excised and incubated with BMOE (8 Å spacer). The products were extracted from the gel slices and analyzed by SDS-PAGE (Figure 3B). Only a faint band corresponding to the MW of the Hin dimer is visible in each of the lanes containing the crosslinked dimer complex (lane 2 of each panel), including the Hin-H107Y control with no introduced cysteines. This very low level of background crosslinking may have arisen from the endogenous Cys28 or perhaps from amines on the Hin surface. Monomeric Hin isolated from the synaptic complexes (lanes 3 and 4) migrates slower than the unreacted monomer (lane 5) because of covalent attachment to the cleaved *hix* DNA. A substantial portion of the crosslinked synaptic complexes from the mutants containing S94C or Q134C migrates as the crosslinked Hin-*hix* conjugate, consistent with the experiments employing labeled DNA above (Figure 2). Therefore, efficient crosslinking requires the formation of the synaptic complex for both regions 1 and 2.

### Uncleaved Synaptic Complexes Are Stabilized by Crosslinks at Region 1

We asked whether crosslinking at regions 1 or 2 could stabilize the Hin-H107Y synaptic complex in the absence of DNA cleavage. Previous experiments have shown that the Hin-DNA covalent linkage is required in order for synaptic complexes to survive gel electrophoresis (Sanders and Johnson, 2004). This result is reproduced in lanes 2 and 6 of Figure 4, which show that Hin-H107Y containing a mutation at the active site residue serine 10 is no longer able to form detectable synaptic complexes with radiolabeled *hix* DNA fragments, although Hin dimer binding to a single *hix* site is unimpaired. When Cys94 is introduced into Hin-H107Y/S10G, a readily detectable amount of synaptic complex is obtained after crosslinking by diamide (0 length), BMOE (8 Å spacer), and, to a lesser extent, BM(PEO)$_4$ (18 Å spacer) (lanes 11–13). The migrations of the uncleaved crosslinked synaptic complexes were indistinguishable from cleaved synaptic complexes formed by Hin-H107Y. Low amounts of uncleaved synaptic complexes were also obtained with Hin-H107Y/S10G/S99C after crosslinking (data not shown). By contrast, crosslinking of Hin-H107Y/S10G/Q134C (lanes 15–17) failed to stabilize the uncleaved synaptic complex. These results are most compatible with region 1 being within the synaptic interface since crosslinks at these positions stabilize synaptic complexes.

### Cleaved Synaptic Complexes Crosslinked at Region 1 Are Competent for DNA Ligation

To evaluate whether cleaved synaptic complexes that are chemically crosslinked remained capable of ligating DNA, cysteine-substituted Hin-H107Y mutants were incubated with radiolabeled DNA, crosslinked with BMH (16 Å spacer), and subjected to native PAGE. Gel slices corresponding to cleaved synaptic complexes were soaked in buffer containing $Mg^{2+}$ to allow ligation, and the products were extracted and analyzed by SDS-

primarily synaptic complexes, with only a small amount of complexes representing Hin dimers bound to a single *hix* site, are obtained (Sanders and Johnson, 2004). Lane 1 contains no Hin, and lane 2 is a reaction with Hin-H107Y (no introduced cysteine).

(B) Results of in-gel crosslinking reactions. Gel slices corresponding to synaptic complexes isolated from native gels as in (A) were excised and incubated with crosslinkers for 30 min. Hin complexes were extracted from the gel matrix and subjected to electrophoresis in SDS-polyacrylamide gels. Panels show the autoradiographs for representative mutants using different crosslinking reagents. The lanes of each panel are labeled with respect to the crosslinker spacer length: lane 1, no crosslinker added; lanes 2 and 3, DTNB and diamide, respectively, to induce direct disulfide linkages; lane 4, BMOE, 8 Å; lane 5, BMB, 11 Å; lane 6, BMH, 16 Å; and lane 7, BM[PEO]$_4$, 18 Å. The locations of monomeric Hin subunits linked to 17 nt cleaved $^{32}$P-labeled DNA (~23.5 kDa) and crosslinked complexes containing two Hin subunits each linked to cleaved DNAs (~47 kDa) are designated on the left of the panels.

(C) Rates of crosslinking in solution. Hin-H107Y/S94C or Q134C were incubated with 3′ $^{32}$P-labeled 36 bp *hix* substrates for 30 min at 37°C to assemble cleavage complexes. BMOE was added for various times (s) as denoted at the top of each panel, followed by quenching with DTT. Synaptic complexes were gel purified as in (A), extracted, and the products electrophoresed in an SDS-polyacrylamide gel.

(D) Results of solution crosslinking reactions with cysteine-substituted Hin-H107Y/C28A mutants. Reactions were performed as in (C) except that different crosslinkers were used, and the crosslinking reaction was for 20 s. Lane 1, no crosslinker; lane 2, diamide, 0 Å; lane 3, BMOE, 8 Å; and lane 4, BMH, 16 Å. The monomeric and crosslinked Hin-DNA conjugates sometimes resolve into doublets, the nature of which is not known.

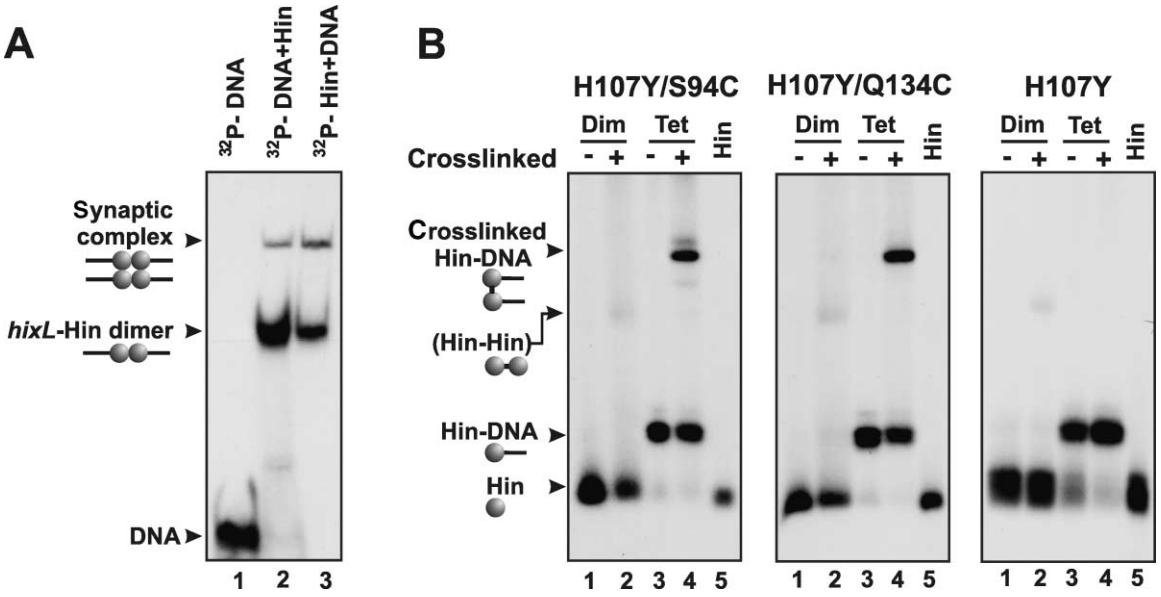


Figure 3. Crosslinking of Hin Dimer and Tetramer Complexes

(A) Native PAGE showing Hin-H107Y dimer and tetramer complexes. Lane 1 is the $^{32}$P-labeled 40 bp *hix* substrate without Hin. Lane 2 is unlabeled Hin-H107Y$^{HMK}$ incubated with the radiolabeled *hix* substrate. Lane 3 is $^{32}$P-labeled Hin-H107Y$^{HMK}$ incubated with unlabeled *hix* substrates. Under these electrophoresis conditions, complexes representing Hin dimers bound to single *hix* sites and synaptic complexes are obtained, and unbound Hin does not enter the gel.

(B) SDS-PAGE of crosslinking reactions. Gel slices corresponding to dimer and tetramer (cleaved synaptic) complexes formed by $^{32}$P-labeled Hin-H107Y$^{HMK}$/S94C or Q134C, as in (A), lane 3, were incubated with BMOE for 5 min, quenched with DTT, and extracted. The crosslinked products, together with noncrosslinked controls, were then subjected to SDS-PAGE. Lanes 1 and 2 of each panel are the noncrosslinked and crosslinked dimer (Dim), and lanes 3 and 4 are the noncrosslinked and crosslinked tetramer (Tet) complexes, respectively. Lane 5 is unreacted $^{32}$P-labeled Hin$^{HMK}$. The locations of monomeric Hin, monomeric Hin-cleaved DNA conjugate, crosslinked Hin dimer (Hin-Hin), and the crosslinked Hin subunits each linked to cleaved DNAs are designated. Note that essentially all the Hin subunits are linked to the cleaved DNA in the tetramer complex but not in the dimer complex.

PAGE (Figure 5). Reactions with Hin-H107Y contained only monomeric Hin linked to the cleaved DNA (lane 9), and these species were efficiently chased into full-length substrate DNA (lane 10), as expected (Sanders and Johnson, 2004). Approximately 90% of the Hin-H107Y/S94C- and S99C-cleaved synaptic complexes were crosslinked (lanes 1 and 3), and these were also efficiently chased into full-length *hix* DNA (lanes 2 and 4).

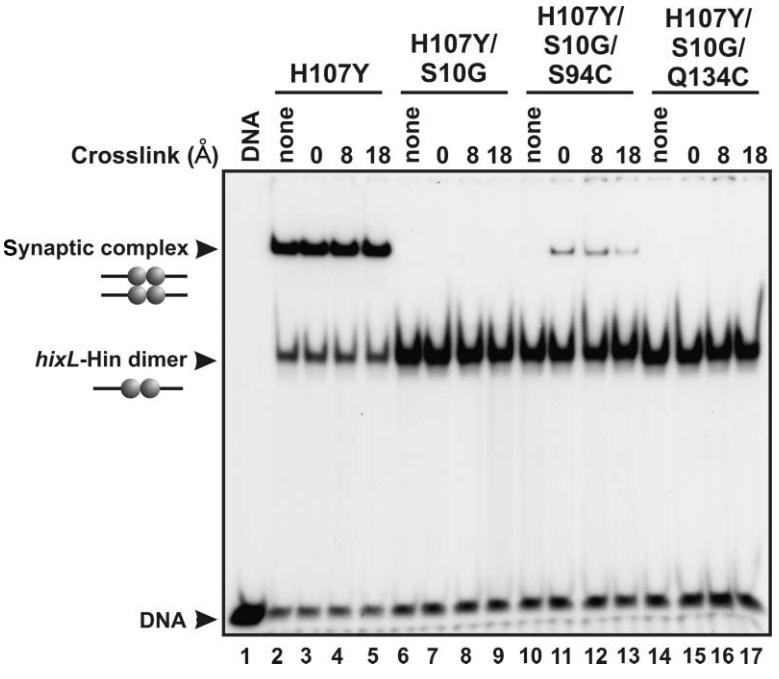


Figure 4. Hin Synaptic Complexes Are Stabilized in the Absence of DNA Cleavage by Crosslinking Residues within Region 1

Hin mutants Hin-H107Y, Hin-H107Y/S10G, Hin-H107Y/S10G/S94C, or Q134C were incubated with radiolabeled 36 bp *hix* substrates for 30 min at 37°C and subjected to crosslinking for 5 min with diamide (0 length) or 1 min with BMOE (8 Å) or BM[PEO]$_4$ (18 Å), as designated. The samples were electrophoresed in a native polyacrylamide gel, and the resulting autoradiograph is shown. The migrations of the dimer and synaptic complex bands along with the unbound DNA are designated. No Hin was added to lane 1.

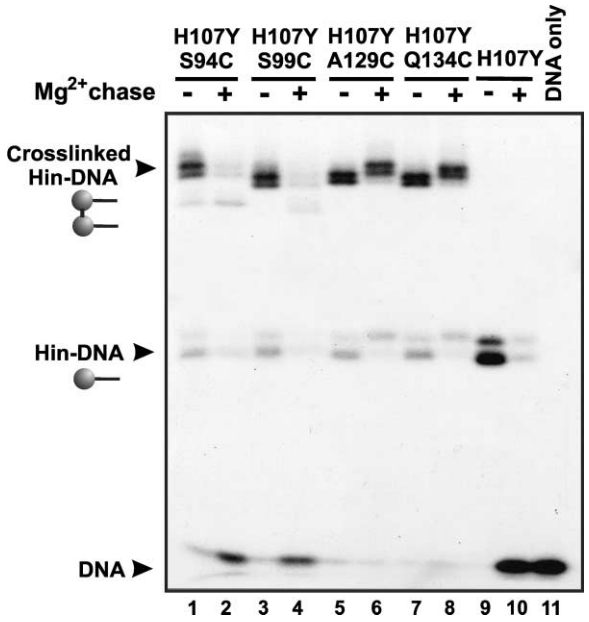


Figure 5. Hin Complexes Crosslinked at Region 1 Remain Competent for Ligation

Cleaved synaptic complexes assembled from Hin-H107Y mutants containing cysteines in region 1 (residues 94 and 99) and region 2 (residues 129 and 134) were crosslinked for 30 min with BMOE (8 Å). The products were electrophoresed in a native polyacrylamide gel, and bands corresponding to cleaved synaptic complexes were excised and either extracted directly in SDS buffer or incubated in 20 mM HEPES (pH 7.5), 10 mM $MgCl_2$, and 10% glycerol for 20 min at 37°C prior to extraction, as designated by the $Mg^{2+}$ chase. The samples were then subjected to SDS-PAGE, and the resulting autoradiograph is shown. Lane 11 contains the unreacted 36 bp DNA substrate. The migrations of the full-length DNA substrate, monomeric Hin-DNA conjugates, and crosslinked Hin-DNA conjugates are denoted. The shift in migration observed for region 2 mutants (lanes 5–8) in the $Mg^{2+}$ chase lanes is not understood.

In contrast, crosslinked Hin-H107Y/A129C and Q134C complexes were unable to reverse the serine-phosphodiester linkage and ligate the DNA (lanes 5–8). We conclude that complexes crosslinked at region 1 remain enzymatically competent, whereas complexes crosslinked in the cleaved configuration at region 2 appear to be trapped in an inactive configuration.

## Hin Subunits Exchange along with the DNA during Recombination

### *Experimental Design*

To define which subunits within the tetrameric synaptic complex are crosslinked and to follow changes that may occur upon DNA exchange, we analyzed complexes formed with different length DNA fragments. As schematically depicted in Figure 6A, there are three potential crosslinked products that could be generated from an initial synaptic complex containing 36 and 112 bp substrates. Crosslinking between Hin subunits of the same dimer (*cis*) will form 17-17 nt or 55-55 nt diprotomers, whereas crosslinking between Hin subunits from different dimers (*trans*) will form 17-55 nt diprotomers. In addition, *trans*-crosslinking could occur in two orientations, direct or diagonal, depending on the alignment of the synapsed dimers and resulting proximity of sulfhydryl groups.

We have shown previously that Hin-H107Y rapidly promotes DNA exchange once it cleaves the DNA (Sanders and Johnson, 2004). Because the DNA ends are covalently associated with the recombinase through the serine-phosphodiester bond, the Hin subunits may exchange together with the DNA. Figure 6B schematically represents the consequences of a coexchange of DNA strands and their linked Hin protomers with respect to the products of cysteine crosslinking. If crosslinking occurs between subunits within the same dimer (*cis*), 17-55 nt diprotomers will be generated after exchange. If *trans*-crosslinking occurs in a direct orientation, no change in the migration of the products will occur upon exchange, as it will give 17-55 nt diprotomers in both cases. However, if *trans*-crosslinking occurs in a diagonal orientation, the products will switch from 17-55 nt diprotomers to 17-17 nt and 55-55 nt diprotomers.

### *Kinetic Analysis of Hin Crosslinking*

Hin-H107Y mutants containing cysteines at region 1 or 2 were incubated with a mixture of 36 and 112 bp *hix* fragments under conditions promoting synaptic complex assembly. At times between 0 and 3 min, samples were incubated with BMOE (8 Å spacer) for 12–20 s followed by addition of excess DTT to quench the crosslinking reaction. Incubation was continued for a total of 30 min to accumulate additional synaptic complexes to facilitate gel isolation. Since the crosslinking reaction is quenched with excess DTT, no change in the crosslinked population will occur during this time. As shown in Figure 6C, the 36/112 bp synaptic complex can be readily separated on native PAGE from the 36/36 bp and 112/112 bp synaptic complexes. The Hin-DNA complexes were then extracted and the crosslinked products resolved by SDS-PAGE.

Figures 6D–6F show the results of time course experiments in which crosslinking reactions were performed on Hin-H107Y/S94C or S99C. To simplify quantitation of the products, the 112 bp substrate was labeled on each 3′ end at a much higher specific activity than the 36 bp substrate. The autoradiograph in Figure 6D illustrates the crosslinked products obtained with 36/112 bp synaptic complexes formed by Hin-H107Y/S94C after 10–80 s of incubation. The graph in Figure 6E displays the percent of 17-55 nt diprotomers among the total crosslinked products. At the early time points, only 17-55 nt diprotomers are present. Within 30–40 s, 55-55 nt diprotomers appear that increase with time and equilibrate at about 40% of the total products after 3 min (the weakly labeled 36-36 nt diprotomer is not visible in the autoradiograph). The results with Hin-H107Y/S99C are similar (Figure 6F). These results indicate that crosslinks at positions 94 and 99 form between subunits of synapsed dimers (*trans*) and that most if not all of the *trans*-crosslinks are in a diagonal orientation. At early time points prior to DNA exchange, only 17-55 nt diprotomers are formed, but, as discussed above, an exchange of subunits between the dimers enables formation of the 55-55 nt diprotomers. The *trans*-crosslinking at positions 94 and 99 confirms region 1 is within the synaptic interface, and the switch to the 55-55 nt diprotomer form demonstrates that DNA exchange is accompanied by an exchange of Hin subunits.

Crosslinking at positions 129 and 134 generates a different kinetic pattern with 36/112 bp synaptic complexes (Figures 6G–6I). At the early time points, where

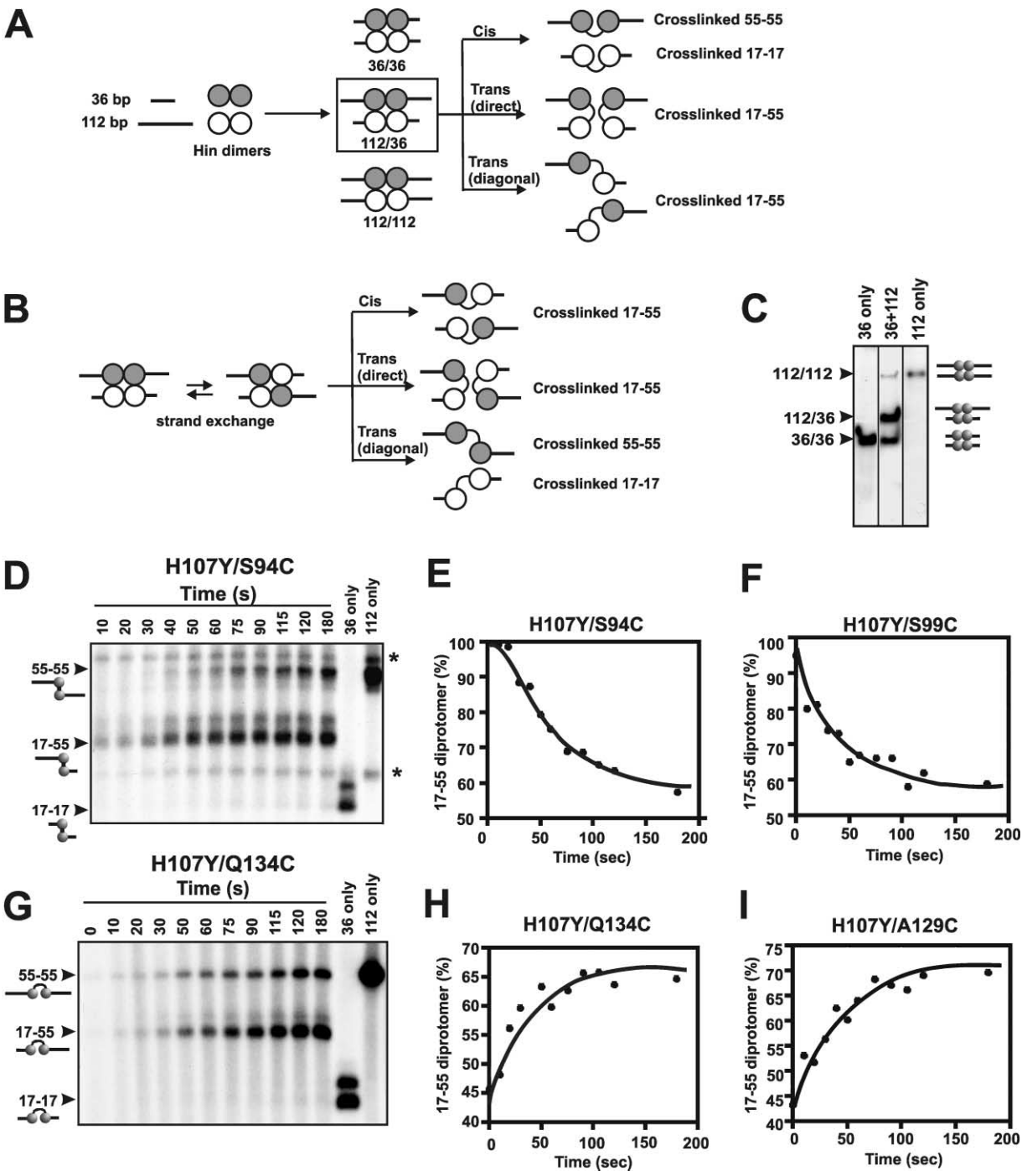


Figure 6. Crosslinking of Synaptic Complexes Formed with Different Length DNA Substrates Demonstrates that Exchange of Hin Subunits Accompanies DNA Exchange

(A) Schematic representation illustrating *cis* or *trans*-crosslinking of complexes formed from different-length DNA substrates. Hin reactions were performed on a mixture of 36 and 112 bp *hix* substrates to assemble 36/36, 36/112, and 112/112 bp synaptic complexes. The possible crosslinked products of 36/112 bp complexes are illustrated; subunits within the same dimer (*cis*) or between different dimers (*trans*) may be linked (see text).

(B) Crosslinking of recombination products within 36/112 bp synaptic complexes where Hin subunits exchange between dimers together with the cleaved DNA molecules. As illustrated in the figure and described in the text, the structure of the products depends on whether the crosslinks form in *cis* or in *trans*.

(C) Separation of synaptic complexes on a native polyacrylamide gel. Hin-H107Y was incubated with radiolabeled 36 bp and/or 112 bp *hix* substrates for 20 min as designated and applied to a 7% polyacrylamide gel containing 10% glycerol. The migrations of the 36/36, 36/112, and 112/112 bp synaptic complexes are shown. The 112 bp substrate is weakly labeled relative to the 36 bp substrate in this experiment.

(D) Crosslinked products formed with increasing incubation times with Hin-H107Y/S94C. Hin-H107Y/S94C was added to a reaction mix containing 3′ $^{32}$P-labeled 112 bp and 36 bp (intentionally radiolabeled at a much lower specific activity) *hix* substrates at 37°C. At times listed

only a small number of crosslinked Hin-DNA products are formed, both 55-55 nt diprotomers and 17-55 nt diprotomers are present, with 55-55 nt diprotomers being slightly overrepresented. The ratio switches with increasing Hin reaction times such that the 17-55 nt diprotomer becomes 65%–70% of the products after 3 min. This pattern indicates that crosslinking in region 2 is occurring between subunits within a single dimer (i.e., in *cis*) and that the Hin subunits are exchanging between synapsed dimers. The presence of both 55-55 and 17-55 nt diprotomers among the region 2 crosslinked products at the early time points suggests that substantial subunit exchange has already occurred. This result is in accordance with earlier conclusions that residues in region 2 can only crosslink after formation of a cleaved synaptic complex and also implies that, once a cleaved complex has been generated, the subunits rapidly exchange between dimers. This conclusion is consistent with previous kinetic analysis of the Hin-H107Y reaction, which found that DNA exchange was rapid relative to the rate of formation of cleaved synaptic complexes (Sanders and Johnson, 2004). Region 1 crosslinks, on the other hand, can occur prior to formation of the cleaved synaptic complex (e.g., Figure 4), and therefore a brief delay in the appearance of exchanged products is not unexpected.

To confirm that subunits are exchanging only within individual recombination complexes and not between different complexes, cleaved synaptic complexes were separately formed with 36 and 112 bp *hix* substrates using Hin-H107Y/S94C or Q134C. The reactions were then mixed and incubated for an additional 5 min prior to crosslinking with BMOE. No 17-55 nt diprotomers were detectable by SDS-PAGE (data not shown). Thus, mixing of subunits between synaptic complexes is not occurring within the time frames of these experiments.

## Discussion

Site-directed protein crosslinking has been used to probe the structure of the Hin synaptic complex and the protein rearrangements that accompany DNA exchange. We find that cysteines located within two regions that are widely separated on the Hin structure support efficient crosslinking. Region 1, where crosslinking occurs between subunits of synapsed dimers in both cleaved and uncleaved synaptic complexes, is centrally located within the top surface of the catalytic domain. Hin tetramers that are covalently linked across the region 1 interface remain competent for ligation, the final enzymatic step of recombination. As elaborated below, the positions of the region 1 crosslinks enable us to model the molecular architecture of the synaptic complex. Crosslinking at residues within region 2, which is located at the C-terminal ends of the E dimerization helices, occurs between residues of subunits from the same dimer that are predicted to be well separated in the Hin apostructure due to the intervening DNA. Region 2 crosslinks only occur in the context of the cleaved synaptic complex and provide evidence for a conformational change in the recombinase that may be a prerequisite for or accompanies DNA cleavage. Kinetic experiments that follow crosslinked products formed at either region 1 or region 2 using differentially tagged Hin dimers provide strong evidence that subunits switch between dimers during DNA recombination.

### Structure of the Synaptic Complex

Figure 7A depicts a surface representation of the Hin dimer, highlighting the locations of cysteines in region 1 (positions 94 and 99; colored red and blue, respectively) that support crosslinking between diagonally opposed subunits of synapsed dimers. Residues in the vicinity where introduced cysteines did not form detectable crosslinks are depicted in green. Positions supporting crosslinking are clustered within the top surface of the catalytic domain surrounding the dimer interface. In Figures 7B and 7C, potential configurations in which Hin catalytic domains could associate with each other in a synaptic complex are considered. In a parallel (Figure 7B) or antiparallel (data not shown) orientation of the catalytic domains, the sulfhydryl groups of cysteines at residues 94 or 99 would not be aligned appropriately to enable 94 to 94 or 99 to 99 crosslinking. However, in a perpendicular orientation (e.g., Figure 7C), residues 94 from each dimer are positioned directly in line with each other and likewise for residues 99. The crosslinked products would be generated, therefore, from *trans*-diagonally oriented pairs of Hin protomers as schematically drawn in Figure 6A and observed experimentally in Fig-

above the autoradiograph, aliquots were subjected to crosslinking for 20 s with 0.4 mM BMOE, followed by incubation in the presence of 40 mM DTT for a total of 30 min to accumulate additional synaptic complexes to facilitate isolation on a native gel as in (C). Synaptic complexes (36/112 bp) were extracted from the native gel and subjected to SDS-PAGE. The autoradiograph of the region of the SDS gel corresponding to the crosslinked Hin-DNA complexes is shown. Products (17-55) corresponding to crosslinked Hin subunits linked to the cleaved 36 bp (17 nt) and 112 bp (55 nt) substrates appear early, whereas products (55-55) corresponding to crosslinked Hin subunits linked to two 55 nt DNAs appear later. Crosslinked Hin subunits linked to two 17 nt DNAs (17-17) are not visible, since the 36 bp substrate was weakly labeled. The lanes on the right side contain the products of crosslinking reactions on separate radiolabeled 36 and 112 bp substrates as reference markers. Two minor species that originate from the 112 bp substrate are designated with an asterisk.

(E) The results of the experiment in (D) with Hin-H107Y/S94C were quantitated and plotted as the percent of the crosslinked 17-55 diprotomer with respect to the total crosslinked products as a function of the time when the 20 s crosslinking reaction was initiated. The calculations considered only the $^{32}P$ labels on both ends of the 112 bp substrate and accounted for the predicted distribution of the labels in the substrates and products.

(F) A similar experiment was performed with Hin-H107Y/S99C and the results are plotted.

(G) Autoradiograph of a crosslinking time course experiment performed using Hin-H107Y/Q134C as in (D), except that the crosslinking reactions were for 12 s.

(H) Graph of the crosslinking results from the experiment in (G) using Hin-H107Y/Q134C.

(I) A similar experiment was performed with Hin-H107Y/A129C, and the results are plotted. Time course experiments have been performed at least twice for each mutant with results in each case similar to those in (D)–(I).

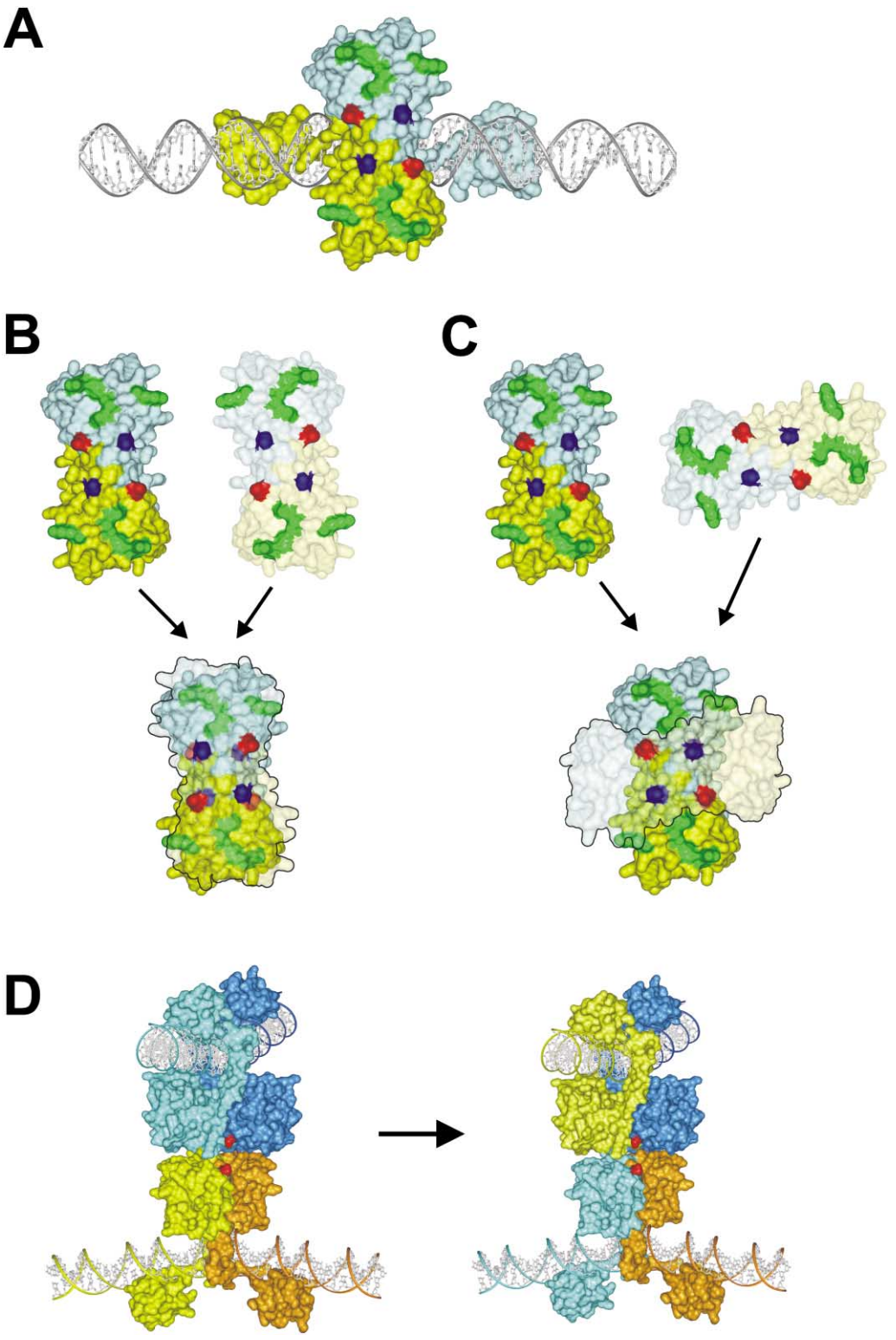


Figure 7. Models of the Hin Synaptic Complex and DNA Exchange by Subunit Rotation

(A) Surface representation of the Hin dimer apostructure model bound to DNA. The view corresponds to a 90° rotation about the x axis of the model depicted in the left panel of Figure 2C. Residues 94 and 99 where crosslinking occurs between diagonally positioned subunits on the synapsed dimer are highlighted in red and blue, respectively. Residues 3, 27, 28, 55, 58, and 89 that did not form crosslinks are colored green.

(B) The catalytic domain in the orientation in (A) and after a 180° rotation about the y axis are shown. These are overlaid to reflect a potential synapsis configuration where the domains are oriented in a parallel configuration, but residues 94 and 99 are not aligned.

(C) The catalytic domain on the right is rotated approximately 90° about the z axis relative to (B). The overlay shows that residues 94 and 99 are aligned over each other, consistent with the crosslinking data.

(D) Model of the Hin synaptic complex that illustrates an exchange of subunits between dimers along with the DNA. The Hin subunits are color coordinated with the *hix* DNA half-site to which they are bound. Ser94 is colored red; Ser99 is not visible because it is buried in the synaptic interface.

ures 6D–6I. In this configuration, the *hix* DNA segments are located on the outside of the complex and oriented near perpendicularly with respect to each other (Figure 7D).

It should be emphasized that simply positioning the apostructures of the dimer models together as depicted in Figures 7C and D does not allow for residues 94 to approach each other closely enough to generate the direct disulfide linkages or even the 8 Å spacer crosslinks that we experimentally observe. Moreover, residues 99 are closer together than those of 94 in the model, yet direct crosslinks between residues 99 do not form. The molecular nature and small surface area of the interface also appears unfavorable for a stable interaction. Therefore, it is likely that changes in the structures of the dimers accompany the formation of a stable synaptic complex even prior to DNA cleavage.

Recent modeling and experimental studies on resolvase have also concluded that DNA is bound on the outside of the synaptic complex (Grindley, 2002). Experimental evidence consistent with a DNA outside model comes from phasing experiments using constrained resolvase substrates where closely spaced recombination sites are juxtaposed by an IHF-induced bend between them (Leschziner and Grindley, 2003). Moreover, mutants of resolvase that form stable tetramers in solution efficiently assemble synaptic complexes, implying that the DNA binding surface is exposed on the outside of a tetrameric core (Sarkis et al., 2001).

### A Structural Change in the E Dimerization Helices Accompanies DNA Cleavage by Hin

In the resolvase dimer apostructure bound to DNA, residues corresponding to Hin positions 129, 132, and 134 are located at the C-terminal end of the extended E helices as they cross the DNA (see Figure 1C). Their side chains are over 30 Å apart on opposite sides of the DNA and therefore would be incapable of crosslinking, even with reagents containing long spacers. Nevertheless, efficient crosslinking by reagents containing 8 Å spacer lengths occurs, and, in the case of residue 129, direct disulfide bonds form between subunits within a DNA bound dimer. Unlike the crosslinks between residues in region 1, region 2 crosslinks have only been observed in the context of a cleaved synaptic complex. These results suggest that the C-terminal ends of the E helices have undergone a conformational change, such as a helix-to-coil transition, prior to or coincident with DNA cleavage by Hin. Unfolding of the C-terminal end of the E helices would remove a steric hindrance that is predicted to interfere with the approach of the active site serines to the labile phosphodiester bonds (Yang and Steitz, 1995) and thus may be a critical regulatory step leading to DNA cleavage by Hin.

Mullen and coworkers have provided NMR evidence that loss of intrinsically unstable E helices of resolvase can lead to repositioning and conformational changes within the remaining folded catalytic center to facilitate DNA attack (Pan et al., 1997, 2001). In addition, crystals of full length or the catalytic domain of $\gamma\delta$ resolvase in the absence of DNA has been reported to be disordered beyond residues 115–122 (Rice and Steitz, 1994a, 1994b; Sanderson et al., 1990). Quaternary changes involving the N-terminal ends of the E helices in the Hin and resolvase dimeric structures upon catalytic activation also have been implicated from previous cysteine crosslinking studies (Haykinson et al., 1996; Hughes et al., 1993; Lim, 1994). Moreover, most of the activating mutations that enable DNA invertases to promote recombination in the absence of Fis are predicted to directly or indirectly affect the dimer interface (Haffter and Bickle, 1988; Johnson, 2002; Klippel et al., 1988).

### Protein and DNA Exchange upon Recombination

The location of the *hix* sites on the outside of the tetrameric protein complex has profound implications for the process of DNA exchange. In this configuration, the core nucleotides where the cleavage-ligation reactions occur are predicted to be separated by over 75 Å. Therefore, a large migration of the cleaved DNA ends from each *hix* site is required to generate a recombinant DNA molecule. We show here that DNA migration is accompanied by a translocation of Hin subunits between dimers. These heterodimers are formed within seconds after Hin cleavage, consistent with the rapid kinetics of DNA exchange measured previously for Hin-H107Y complexes after the rate-limiting cleavage step (Sanders and Johnson, 2004). The heterodimers can be crosslinked either at region 1 or region 2, implying that the entire subunit is translocating. Specifically, the heterodimeric crosslinks at region 2 indicate that the E helix is translocating, which is not compatible with the "domain swapping" model for recombination where the catalytic domain is proposed to translocate independently of the E helix dimerization region (Burke et al., 2004; Grindley, 2002). The finding that the heterodimers efficiently form under metal-free reaction conditions also is contrary to a recent report that proposed that $Mg^{2+}$ was required for DNA strand exchange (Lee et al., 2003).

Recombination mediated by an exchange of protein subunits is compatible with earlier DNA topological studies with wild-type Hin and other serine recombinases using plasmid substrates (Heichman et al., 1991; Kanaar et al., 1988, 1990; Merickel and Johnson, 2004; Stark et al., 1989, 1991). These experiments indicated that the DNA strands undergo one or, under certain conditions, multiple rotations about each other upon recombination, which leads to a defined loss of DNA supercoils or the conversion of DNA supercoils into knot or catenane nodes. Since the recombinase subunits are covalently linked to the DNA ends, concurrent rotations of the recombinase subunits were strongly implied.

A subunit rotation mechanism for DNA strand exchange by serine recombinases fundamentally differs from the "single-strand swapping" mechanism that characterizes the tyrosine recombinase reactions (Nunes-Duby et al., 1995). The distinct reaction mechanisms follow from the opposing architectures of the recombination complexes. Strand exchange by tyrosine recombinases is accomplished in a multistep process that involves sequential sets of single-strand DNA cleavage-ligation reactions within a Holliday intermediate. The recombining DNA strands are located relatively close to each other within the center of a tetrameric recombinase core, and only a modest conformational adjustment is required to reposition the recombinase catalytic sites

between the two DNA cleavage-ligation steps (Chen et al., 2000; Gopaul et al., 1998; Guo et al., 1997). In contrast, DNA exchange by serine recombinases is a more concerted reaction whereby all four DNA strands are cleaved and then translocated over long distances by an exchange of recombinase subunits between dimers.

## Experimental Procedures

### Cloning and Purification of Hin Mutants

The Hin mutants were typically constructed by two-step PCR reactions using the Hin-H107Y gene as a template and were cloned into pET11a (Novagen). Hin-H107Y/N27C contained an unintentional proline substitution at Cys28. Hin proteins were purified from renatured inclusion bodies as described (Sanders and Johnson, 2004). All of the cysteine-containing Hin mutants reported in this paper, including Hin-H107Y/N27C/C28P, efficiently assembled cleaved synaptic complexes and catalyzed recombination in vitro. However, preparations of mutants containing the C28A mutation gave reproducibly lower yields and were less stable.

### Hin Crosslinking Reactions

Cleaved synaptic complexes were assembled as described in Sanders and Johnson [2004]. In brief, 3–5 pmoles of Hin-H107Y mutants, which were prereduced by incubation overnight with 10 mM DTT, were incubated with 0.3–0.4 pmoles of 3′ $^{32}$P-labeled *hix* substrates (see below) in a 25 μl reaction mix containing 20 mM HEPES (pH 7.5), 80 mM NaCl, 4 mM CHAPS, 0.4 μg/μl poly-glutamate, and 25% ethylene glycol for 20–30 min at 37°C. For in-gel crosslinking, the reactions were applied to an 8% polyacrylamide (19:1 acrylamide: bisacrylamide) gel with or without 10% glycerol and electrophoresed in 0.5 × TBE. The gels were exposed to X-ray film, and bands of interest were excised and soaked for 5–30 min at 37°C in a solution containing 10 mM HEPES (pH 7.5), 1 mM EDTA, 10% glycerol (buffer A), and 0.3 mM crosslinker. The solution was then replaced with buffer A containing 30 mM DTT (no DTT when diamide or DTNB were used) for 5 min. The gel slices were crushed and eluted in 150 μl 10 mM HEPES (pH 7.5), 1 mM EDTA, and 1% SDS (buffer B). The supernatant was recovered by centrifugation, mixed with SDS loading dye, and heated at 70°C for 2 min, and aliquots were loaded onto a 10% or 12.5% polyacrylamide (29:1 acrylamide:bisacrylamide) gel containing 0.2% SDS and electrophoresed in Tris-Glycine buffer containing 0.2% SDS. The dried gels were imaged and quantified using a phosphorimager and ImageQuant software (Amersham). For solution crosslinking, Hin reactions were incubated directly with 0.4 mM crosslinker for varying times (typically 20 s) at 37°C. Bismaleimide crosslinking reactions were quenched with 40 mM DTT, and diamide and DTNB samples were placed on ice prior to electrophoresis in native polyacrylamide gels containing 10% glycerol. Bands corresponding to synaptic complexes were excised and extracted in buffer B, and the Hin-DNA complexes were analyzed by SDS-PAGE as described above.

Cysteines were oxidized to promote direct disulfide bonds using diamide or 5,5′-dithiobis (2-nitrobenzoic acid) (DTNB) obtained from Sigma. Cysteine-specific crosslinkers (Pierce) with varying spacer lengths between sulfhydryl reactive groups used were the following: *bis*-maleimidoethane (BMOE, 8 Å), *bis*-maleimidobutane (BMB, 11 Å), *bis*-maleimidohexane (BMH, 16 Å), and 1,11-bis-maleimidotetraethyleneglycol (BM[PEO]$_4$, 18 Å). All crosslinkers were dissolved at 10 mM concentration in DMSO.

DNA substrates were prepared as follows. Most experiments were performed on 36 or 40 bp synthetic oligonucleotides containing the 26 bp *hixL* sequence. The 36 bp substrate was 3′ end labeled by reacting each stand with terminal deoxynucleotidyl transferase (New England Biolabs) and cordycepin 5′-triphosphate-3′[$^{32}$P] (Perkin-Elmer). The strands were then mixed; chromatographed through a DyeEx 2.0 spin column (Qiagen) in 20 mM Tris (pH 8.0), 1 mM EDTA, and 100 mM NaCl; and annealed by heating and slow cooling. Duplexes were purified on native polyacrylamide gels. The 40 bp substrate was prepared by annealing synthetic oligonucleotides, which generated 4 nt 3′ extensions that represented EcoRI recognition sequences on both ends. The ends were filled in using Klenow and α $^{32}$P-dATP, and the labeled duplex DNA was gel-purified. The 112 bp substrate with a centrally located *hixL* site was synthesized by PCR using primers that contained terminally located EcoRI sites. The products of the PCR reaction were digested with EcoRI, end filled with Klenow and α $^{32}$P-dATP, and gel purified. Hin$^{HMK}$ mutants were constructed and labeled using heart muscle kinase and γ $^{32}$P-ATP as described previously (Sanders and Johnson, 2004).

## Acknowledgments

We thank Stacy Merickel for isolation and initial characterization of Hin mutants, Catherine Sohn and Daniel Yoo for assistance in purification of Hin mutants, and Muriel Laine for early work on the project. This work was supported by NIH grant GM38509.

Received: June 19, 2004
Revised: August 17, 2004
Accepted: August 19, 2004
Published: September 30, 2004

## References

Burke, M.E., Arnold, P.H., He, J., Wenwieser, S.V.C.T., Rowland, S.-J., Boocock, M.R., and Stark, W.M. (2004). Activating mutations of Tn3 resolvase marking interfaces important in recombination catalysis and its regulation. Mol. Microbiol. *51*, 937–948.

Chen, Y., Narendra, U., Iype, L.E., Cox, M.M., and Rice, P.A. (2000). Crystal structure of a FLP recombinase-Holliday junction complex: assembly of an active oligomer by helix swapping. Mol. Cell *6*, 885–897.

Chiu, T.K., Sohn, C., Dickerson, R.E., and Johnson, R.C. (2002). Testing water-mediated DNA recognition by the Hin recombinase. EMBO J. *21*, 801–814.

Craig, N.L., Craigie, R., Gellert, M., and Lambowitz, A.M. (2002). Mobile DNA II (Washington, D.C.: ASM Press).

Gopaul, D.N., Guo, F., and Van Duyne, G.D. (1998). Structure of the Holliday junction intermediate in Cre-*loxP* site-specific recombination. EMBO J. *17*, 4175–4187.

Grindley, N.D.F. (2002). The movement of Tn*3*-like elements: transposition and cointegrate resolution. In Mobile DNA II, N.L. Craig, R. Craigie, M. Gellert, and A.M. Lambowitz, eds. (Washington, D.C.: ASM Press), pp. 272–302.

Guo, F., Gopaul, D.N., and van Duyne, G.D. (1997). Structure of Cre recombinase complexed with DNA in a site-specific recombination synapse. Nature *389*, 40–46.

Haffter, P., and Bickle, T.A. (1988). Enhancer-independent mutants of the Cin recombinase have a relaxed topological specificity. EMBO J. *7*, 3991–3996.

Haykinson, M.J., Johnson, L.M., Soong, J., and Johnson, R.C. (1996). The Hin dimer interface is critical for Fis-mediated activation of the catalytic steps of site-specific DNA inversion. Curr. Biol. *6*, 163–177.

Heichman, K.A., and Johnson, R.C. (1990). The Hin invertasome: protein-mediated joining of distant recombination sites at the enhancer. Science *249*, 511–517.

Heichman, K.A., Moskowitz, I.P., and Johnson, R.C. (1991). Configuration of DNA strands and mechanism of strand exchange in the Hin invertasome as revealed by analysis of recombinant knots. Genes Dev. *5*, 1622–1634.

Hughes, R.E., Rice, P.A., Steitz, T.A., and Grindley, N.D. (1993). Protein-protein interactions directing resolvase site-specific recombination: a structure-function analysis. EMBO J. *12*, 1447–1458.

Jayaram, M., Grainge, I., and Tribble, G. (2002). Site-specific recombination by the FLP protein of *Saccharomyces cerevisiae*. In Mobile DNA II, N.L. Craig, R. Craigie, M. Gellert, and A.M. Lambowitz, eds. (Washington, D.C.: ASM Press), pp. 192–218.

Johnson, R.C. (2002). Bacterial site-specific DNA inversion systems. In Mobile DNA II, N.L. Craig, R. Craigie, M. Gellert, and A.M. Lambowitz, eds. (Washington, D.C.: ASM Press), pp. 230–271.

Johnson, R.C., and Simon, M.I. (1985). Hin-mediated site-specific

recombination requires two 26 bp recombination sites and a 60 bp recombinational enhancer. Cell *41*, 781–791.

Johnson, R.C., Bruist, M.F., and Simon, M.I. (1986). Host protein requirements for in vitro site-specific DNA inversion. Cell *46*, 531–539.

Johnson, R.C., Glasgow, A.C., and Simon, M.I. (1987). Spatial relationship of the Fis binding sites for Hin recombinational enhancer activity. Nature *329*, 462–465.

Kanaar, R., van de Putte, P., and Cozzarelli, N.R. (1988). Gin-mediated DNA inversion: product structure and the mechanism of strand exchange. Proc. Natl. Acad. Sci. USA *85*, 752–756.

Kanaar, R., Klippel, A., Shekhtman, E., Dungan, J.M., Kahmann, R., and Cozzarelli, N.R. (1990). Processive recombination by the phage Mu Gin system: implications for the mechanisms of DNA strand exchange, DNA site alignment, and enhancer action. Cell *62*, 353–366.

Klippel, A., Cloppenborg, K., and Kahmann, R. (1988). Isolation and characterization of unusual Gin mutants. EMBO J. *7*, 3983–3989.

Lee, H.J., Lee, Y.L., Ji, J.J., and Lim, H.M. (2003). The effects of ethidium bromide and $Mg^{++}$ ion on strand exchange in the Hin-mediated inversion reaction. Mol. Cells *16*, 377–384.

Leschziner, A.E., and Grindley, N.D.F. (2003). The architecture of the gamma delta resolvase crossover site synaptic complex revealed by using constrained DNA substrates. Mol. Cell *12*, 775–781.

Lim, H.M. (1994). Analysis of subunit interaction by introducing disulfide bonds at the dimerization domain of Hin recombinase. J. Biol. Chem. *269*, 31134–31142.

Merickel, S.K., and Johnson, R.C. (2004). Topological analysis of Hin-catalysed DNA recombination in vivo and in vitro. Mol. Microbiol. *51*, 1143–1154.

Merickel, S.K., Haykinson, M.J., and Johnson, R.C. (1998). Communication between Hin recombinase and Fis regulatory subunits during coordinate activation of Hin-catalyzed site-specific DNA inversion. Genes Dev. *12*, 2803–2816.

Nunes-Duby, S.E., Azaro, M.A., and Landy, A. (1995). Swapping DNA strands and sensing homology without branch migration in lambda site-specific recombination. Curr. Biol. *5*, 139–148.

Pan, B., Deng, Z., Liu, D., Ghosh, S., and Mullen, G.P. (1997). Secondary and tertiary structural changes in gamma delta resolvase: comparison of the wild-type enzyme, the I110R mutant, and the C-terminal DNA binding domain in solution. Protein Sci. *6*, 1237–1247.

Pan, B., Maciejewski, M.W., Marintchev, A., and Mullen, G.P. (2001). Solution structure of the catalytic domain of gamma delta resolvase. Implications for the mechanism of catalysis. J. Mol. Biol. *310*, 1089–1107.

Rice, P. (2002). Theme and variation in tyrosine recombinases: structure of a FLP-DNA complex. In Mobile DNA II, N.L. Craig, R. Craigie, M. Gellert, and A.M. Lambowitz, eds. (Washington, D.C.: ASM Press), pp. 219–229.

Rice, P.A., and Steitz, T.A. (1994a). Model for a DNA-mediated synaptic complex suggested by crystal packing of gamma delta resolvase subunits. EMBO J. *13*, 1514–1524.

Rice, P.A., and Steitz, T.A. (1994b). Refinement of gamma delta resolvase reveals a strikingly flexible molecule. Structure *2*, 371–384.

Sanders, E.S., and Johnson, R.C. (2004). Stepwise dissection of the Hin-catalyzed recombination reaction from synapsis to resolution using oligonucleotide substrates. J. Mol. Biol. *340*, 753–766.

Sanderson, M.R., Freemont, P.S., Rice, P.A., Goldman, A., Hatfull, G.F., Grindley, N.D., and Steitz, T.A. (1990). The crystal structure of the catalytic domain of the site-specific recombination enzyme gamma delta resolvase at 2.7 Å resolution. Cell *63*, 1323–1329.

Sarkis, G.J., Murley, L.L., Leschziner, A.E., Boocock, M.R., Stark, W.M., and Grindley, N.D.F. (2001). A model for the gamma delta resolvase synaptic complex. Mol. Cell *8*, 623–631.

Silverman, M., Zieg, J., Mandel, G., and Simon, M. (1981). Analysis of the functional components of the phase variation system. Cold Spring Harb. Symp. Quant. Biol. *45*, 17–26.

Stark, W.M., Sherratt, D.J., and Boocock, M.R. (1989). Site-specific recombination by Tn*3* resolvase: topological changes in the forward and reverse reactions. Cell *58*, 779–790.

Stark, W.M., Grindley, N.D., Hatfull, G.F., and Boocock, M.R. (1991). Resolvase-catalysed reactions between *res* sites differing in the central dinucleotide of subsite I. EMBO J. *10*, 3541–3548.

Van Duyne, G.D. (2002). A structural view of tyrosine recombinase site-specific recombination. In Mobile DNA II, N.L. Craig, R. Craigie, M. Gellert, and A.M. Lambowitz, eds. (Washington, D.C.: ASM Press), pp. 93–117.

Yang, W., and Steitz, T.A. (1995). Crystal structure of the site-specific recombinase gamma delta resolvase complexed with a 34 bp cleavage site. Cell *82*, 193–207.

Zieg, J., Silverman, M., Hilmen, M., and Simon, M. (1977). Recombinational switch for gene expression. Science *196*, 170–172.